Strings as Multi–Particle States of Quantum σ–Models

Nikolay Gromov[a,b], Vladimir Kazakov[a], Kazuhiro Sakai[a], Pedro Vieira[a,c]

[a] LPT de l'Ecole Normale Supérieure et Université Paris-VI, Paris
[b] St.Petersburg INP, Gatchina, 188 300, St.Petersburg
[c] CFP and Departamento de Física, Faculdade de Ciências Universidade do Porto.

1 On the one hand...

The fundamental quantum excitations of the $O(4)$ sigma–model

$$S=\frac{\sqrt{\lambda}}{4\pi}\int_0^{2\pi} d\sigma \int d\tau \,(\partial_a X_i)^2 \quad , \quad X_i X_i = 1\,, \qquad (1)$$

are particles with dynamically generated mass, momentum $p(\theta) = \frac{\mu}{2\pi}\sinh \pi\theta$ and $SO(4) = SU(2)\times SU(2)$ isotopic degree of freedom.

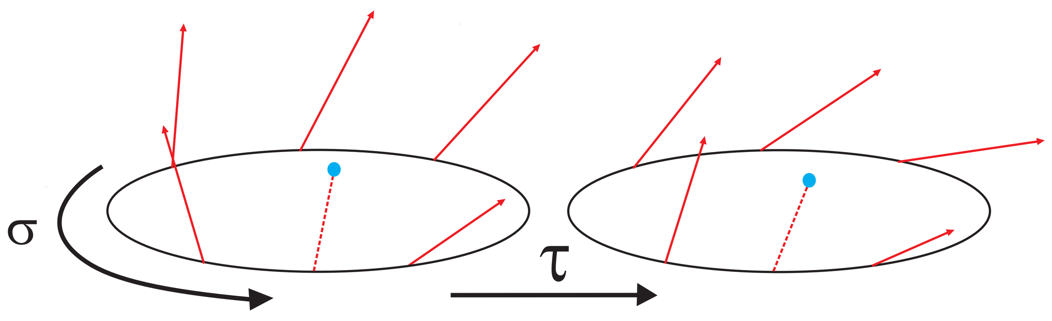

Fig. 1: Each particle in the σ circle carries an isotopic $SO(4)$ degree of freedom, parametrized by a four dimensional unit vector.

The many–particle wave function will depend of the momenta $p(\theta)$ conjugate to σ and on the momenta of the spin waves of both the $SU(2)$ isotopic degrees of freedom (parametrized by u and v). Periodicity of the wave function in the circle of length 2π yields the Bethe ansatz (BA) equations

$$e^{-i\mu\sinh\pi\theta_\alpha} = \prod_{\beta\neq\alpha}^{L} S_0^2(\theta_\alpha-\theta_\beta)$$
$$\prod_{j}^{J_u}\frac{\theta_\alpha-u_j+i/2}{\theta_\alpha-u_j-i/2}\prod_{k}^{J_v}\frac{\theta_\alpha-v_k+i/2}{\theta_\alpha-v_k-i/2},$$
$$1=\prod_{\beta}^{L}\frac{u_j-\theta_\beta-i/2}{u_j-\theta_\beta+i/2}\prod_{i\neq j}^{J_u}\frac{u_j-u_i+i}{u_j-u_i-i},$$
$$1=\prod_{\beta}^{L}\frac{v_k-\theta_\beta-i/2}{v_k-\theta_\beta+i/2}\prod_{l\neq k}^{J_v}\frac{v_k-v_l+i}{v_k-v_l-i}.$$

The explicit form of the scalar factor S_0 is known. For large rapidities, $i\log S_0^2(\theta)\simeq 1/\theta + \mathcal{O}\left(\theta^{-3}\right)$.

In the classical limit the *quantum* generated mass μ is very small. Taking the *log* of BA eqs and rescaling

$$(\theta,u,v)\to -\frac{\log\mu}{2\pi}(\theta,u,v)\,,$$

one obtains a set of equations which resemble the equilibrium conditions for the positions θ_α, u_i and v_k of three species of interacting particles. Furthermore the particles θ's feel an external potential.

$$V(\theta)=\mu\cosh\left(\frac{\log\mu}{2}\theta\right)$$

which tends, as $\mu\to 0$, to the box potential. We can replace it by adequate boundary conditions at $\theta=\pm 2$.

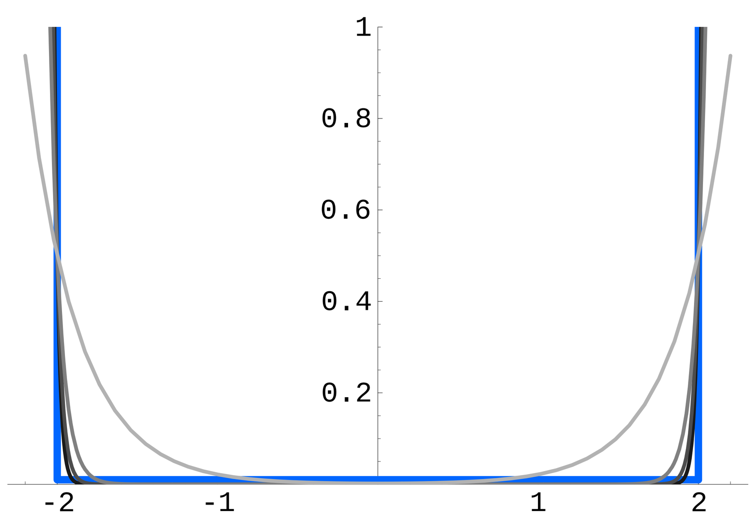

Fig. 2: We plot $V(\theta)$ for $-\frac{\log\mu}{2\pi}=1,5,9,13$ (lighter to darker gray).

For large L, J_u, J_v the particles will condense into curves, cuts $\mathcal{C}$ in the complex plane, described by

$$\begin{aligned} 2\,\not{G}_u(z)-G_\theta(z) &= 2\pi n_u, & z\in\mathcal{C}_u\\ \not{G}_\theta(z)-G_v(z)-G_u(z) &= -2\pi m, & z\in\mathcal{C}_\theta\\ 2\,\not{G}_v(z)-G_\theta(z) &= 2\pi n_v, & z\in\mathcal{C}_v\end{aligned}\qquad (2)$$

where $G_\theta(z)\equiv -\frac{2\pi}{\log\mu}\sum_{\beta=1}^{L}\frac{1}{z-\theta_\beta}$ (with similar definitions for G_u and G_v) and $\not{G}$ is the average of the resolvent above and below the cut. Furthermore we consider a single mode number for all θ's. Let

$$p_1=-p_2=G_u-\frac{1}{2}G_\theta\ ,\ \ p_3=-p_4=G_v-\frac{1}{2}G_\theta\,.$$

The crucial remark is that equations (2) translate into the statement that the quasi-momenta $p_1'(z), p_2'(z), p_3'(z), p_4'(z)$ form the four sheets of the Riemann surface of an analytical function $p'(z)$.

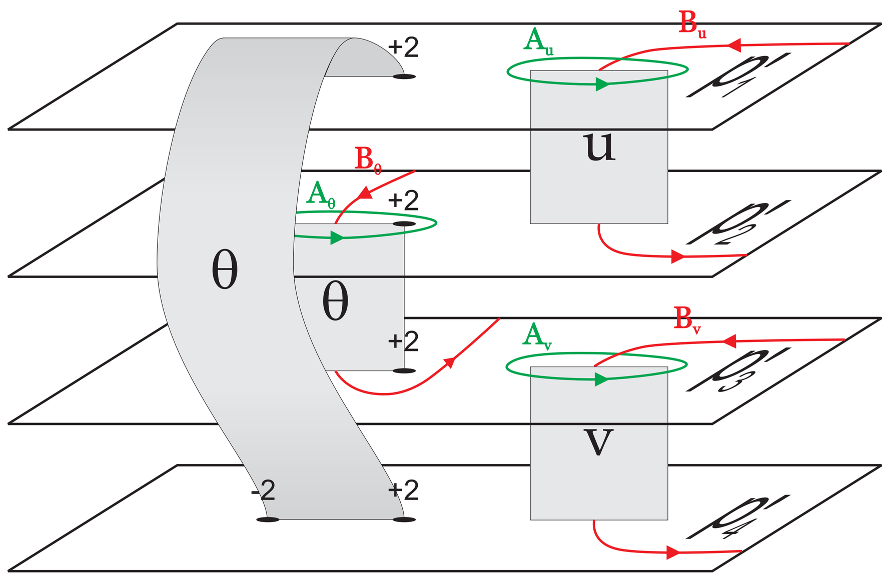

Fig. 3: Structure of the curve coming from the Bethe ansatz side.

2 ... on the other hand

Action (1) also describes the movement of a closed string in a 3–sphere.

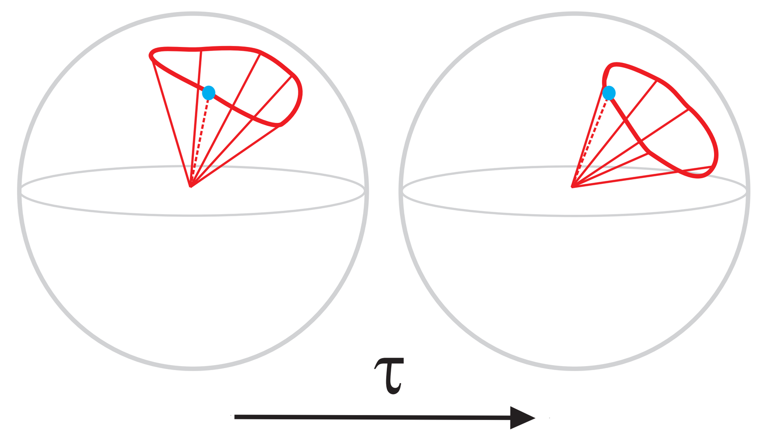

Fig. 4: Each particle in figure 1 is mapped into a point of the string. The descritised string becomes continuous in the limit of large number of particles.

Let us ensemble the string coordinates in the $SU(2)$ element $g = X_1 + i\sigma_3 X_2 + i\sigma_2 X_3 + i\sigma_1 X_4$. From the pure gauge current $j = g^{-1}dg$ we construct

$$J_\tau(x)=\frac{x\,j_\tau+j_\sigma}{x^2-1}\quad,\quad J_\sigma(x)=\frac{x\,j_\sigma+j_\tau}{x^2-1}$$

where x is a generic complex number called the spectral parameter. The equations of motion and the definition of j imply that, for *all* x,

$$[\partial_\tau - J_\tau(x), \partial_\sigma - J_\sigma(x)] = 0\,.$$

Then

$$\cos\tilde{p}(x)\equiv T(x)\equiv\frac{1}{2}\mathrm{Tr}\left(\overleftarrow{P}\exp\int_0^{2\pi}d\sigma\, J_\sigma(x)\right)$$

is τ independent. This provides us an infinite set of conserved charges. Apart from the essential singularities at $x=\pm 1$, $T(x)$ is an analytical function in the x–complex plane. At $x=\pm 1$ the quasimomentum $\tilde{p}(x)$ has poles whose residues are fixed by the Virasoro constraints. Finally, since

$$\tilde{p}'(x)=-\frac{T'(x)}{\sqrt{1-T^2(x)}}$$

$\tilde{p}'(x)$ will define a 2–sheet Riemann surface with branch points where $T(x)=\pm 1$.

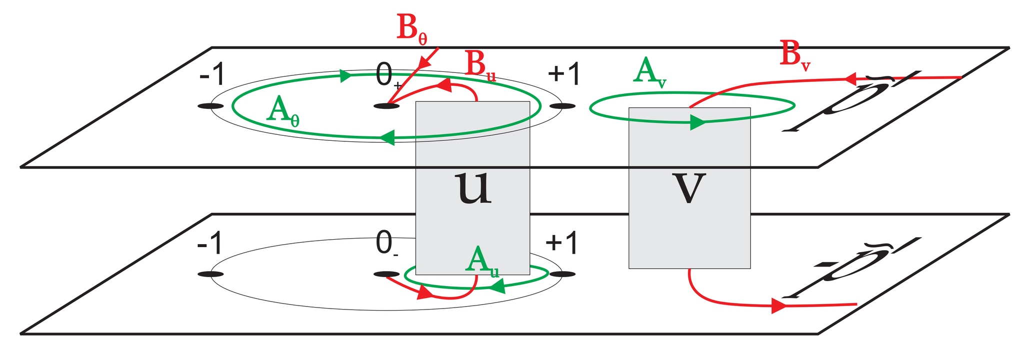

Fig. 5: Algebraic curve from the finite gap method.

3 Fusion

Each of the previous sections ended with a plot of a Riemann surface. These encoded the positions of the roots of the system of BA eqs. in the classical limit (figure 3) and the analytical properties of the quasimomentum associated with each classical solution (figure 5). The main statement of our work is that these Riemann surfaces are different projections of the same object.

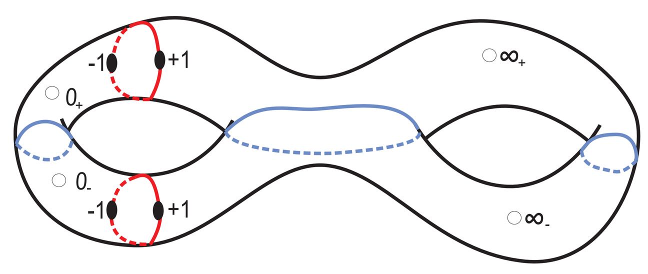

Fig. 6: The curves appearing from the finite gap method and the BA equations turn out to the different projection of the same curve.

The key tool is the Zhukovsky map

$$z = x+\frac{1}{x}\,.$$

Let us mention two properties of this map. Firstly it maps

$$\frac{1}{\sqrt{z\pm 2}}\longleftrightarrow\frac{1}{x\pm 1}\,.$$

In the BA context the left hand side appears as the asymptotic behavior of the resolvent (or of the density) of the θ particles close to the walls of the box at $z=\pm 2$. In the string context the poles at $x=\pm 1$ are present by construction. What happens then is that poles at ± 1 of figure 5 are mapped to the θ cuts of figure 3.

The second crucial property is that the interior (or exterior) of the unit circle in the x–plane is mapped into a full z–plane. Thus the Zhukovsky map doubles the number of sheets. More precisely, the two upper sheets of figure 3, with u-cuts, are mapped into the interior of the unit circle in the x projection while the two lower sheets are projected into the exterior of the unit circle.

4 Acknowledgments

V.K. was partially supported by European Union under the RTN contracts MRTN-CT-2004-512194 and by INTAS-03-51-5460 grant. N.G. was partially supported by French Government PhD fellowship and by RSGSS-1124.2003.2. P. V. is funded by the Fundação para a Ciência e Tecnologia SFRH/BD/17959/2004/0WA9.

5 References

References in [hep-th/0603043].